

# The dual role of dendritic cells in the immune response to human immunodeficiency virus type 1 infection

Ian B. Hogue,<sup>1</sup> Seema H. Bajaria,<sup>1†</sup> Beth A. Fallert,<sup>2</sup> Shulin Qin,<sup>2</sup> Todd A Reinhart<sup>2</sup> and Denise E. Kirschner<sup>1</sup>

Correspondence  
Denise E. Kirschner  
kirschne@umich.edu

<sup>1</sup>Department of Microbiology and Immunology, The University of Michigan Medical School, Ann Arbor, MI, USA

<sup>2</sup>Department of Infectious Diseases and Microbiology, Graduate School of Public Health, University of Pittsburgh, Pittsburgh, PA, USA

Many aspects of the complex interaction between human immunodeficiency virus type 1 (HIV-1) and the human immune system remain elusive. Our objective was to study these interactions, focusing on the specific roles of dendritic cells (DCs). DCs enhance HIV-1 infection processes as well as promote an antiviral immune response. We explored the implications of these dual roles. A mathematical model describing the dynamics of HIV-1, CD4<sup>+</sup> and CD8<sup>+</sup> T-cells, and DCs interacting in a human lymph node was analysed and is presented here. We have validated the behaviour of our model against non-human primate simian immunodeficiency virus experimental data and published human HIV-1 data. Our model qualitatively and quantitatively recapitulates clinical HIV-1 infection dynamics. We have performed sensitivity analyses on the model to determine which mechanisms strongly affect infection dynamics. Sensitivity analysis identifies system interactions that contribute to infection progression, including DC-related mechanisms. We have compared DC-dependent and -independent routes of CD4<sup>+</sup> T-cell infection. The model predicts that simultaneous priming and infection of T cells by DCs drives early infection dynamics when activated T-helper cell numbers are low. Further, our model predicted that, while direct failure of DC function and an indirect failure due to loss of CD4<sup>+</sup> T-helper cells are both significant contributors to infection dynamics, the former has a more significant impact on HIV-1 immunopathogenesis.

Received 19 November 2007  
Accepted 25 April 2008

## INTRODUCTION

Despite advances in our understanding of human immunodeficiency virus type 1 (HIV-1) and the human immune response in the last 25 years, much of this complex interaction remains elusive. CD4<sup>+</sup> T-cells are targets of HIV-1, and are also important for the establishment and maintenance of an adaptive immune response (Poli *et al.*, 1993). CD8<sup>+</sup> T-cells are the primary effector cells in HIV-1 infection, as they kill infected cells and produce non-lytic antiviral factors. In lymph nodes (LNs), myeloid dendritic cells (DCs) serve as antigen presenting cells, activating CD4<sup>+</sup> and CD8<sup>+</sup> T-cells (Steinman, 1991). Despite the ‘DC’ moniker, follicular DCs are functionally different from myeloid DCs; therefore, we did not consider follicular DCs in our model. Another class that was not considered here was plasmacytoid DCs, which are noted for their high production of interferon, but are less potent antigen presenting cells. DCs

are also of particular importance because HIV-1 exploits DCs to enhance infection (Lekkerkerker *et al.*, 2006). Thus, DCs are a critical link between virus, CD4<sup>+</sup> and CD8<sup>+</sup> T-cells (Fig. 1). Elucidating the mechanisms of DC–virus interactions is crucial in uncovering more details about host–virus dynamics during HIV-1 infection. Toward this goal, we developed a mathematical model of HIV-1 dynamics within a human LN, as it is the major site of viral replication and generation of the antiviral immune response.

The prototypical ‘Langerhans cell paradigm’ behaviour of DCs is that, after encountering antigen in the periphery, DCs mature and travel to the LN (Wilson & Villadangos, 2004). DC maturation includes increasing antigen presentation on major histocompatibility complex (MHC) molecules, and upregulating co-stimulatory molecules (Steinman, 1991). Mature DCs prime CD4<sup>+</sup> T-cells to become effector T-helper cells. Additionally, DCs cross-present exogenous antigens on MHC class I to prime CD8<sup>+</sup> T-cells. Primed CD8<sup>+</sup> T-cells differentiate into

<sup>†</sup>Present address: Entelos, Inc., 110 Marsh Drive, Foster City, CA, USA.



enhanced by DCs, showing that the relative importance of this effect changes with respect to infection state. In particular, our model predicts which mechanisms of DC dysfunction are most significant in the transition to AIDS.

## METHODS

**NHP SIV infection model.** Adult cynomolgus macaques (*Macaca fascicularis*) were infected intrarectally with SIV/DeltaB670 (Murphey-Corb *et al.*, 1986) and sacrificed at 2 weeks post-infection or upon development of AIDS, defined by reduced CD4<sup>+</sup> T-cell counts and clinical symptoms. Axillary and hilar LN tissues were processed as described previously (Fallert & Reinhart, 2002; Reinhart *et al.*, 2002). The animal studies were performed under the guidance and approval of the University of Pittsburgh Institutional Animal Care and Use Committee.

**Immunofluorescence microscopy and immunohistochemistry.** We performed immunofluorescence on 14 µm tissue sections using primary antibodies for Ki67 (clone MM1, 1:100; Novocastra) and CD3 (clone CD3-12, 1:100; Novocastra), secondary antibodies fluorescein isothiocyanate (FITC)-conjugated goat anti-mouse IgG1 (1:100; Jackson ImmunoResearch), biotinylated goat anti-rabbit Ig (1:100; Zymed), AF488-conjugated rabbit anti-fluorescein (1:80; Molecular Probes) and streptavidin-AF647 (1:100; Molecular Probes). Images were captured on an Olympus Fluoview 500 laser scanning confocal microscope. Images were analysed using MetaMorph software (Universal Imaging). CD3 is a marker for T-cells, and Ki67 indicates cells that have divided within the past 3–4 days (Pitcher *et al.*, 2002). Because T-cell division during HIV-1 infection is primarily due to antigen-driven immune activation rather than an antigen-independent homeostatic response (Cohen Stuart *et al.*, 2000; Hazenberg *et al.*, 2000), we considered CD3<sup>+</sup>Ki67<sup>+</sup> cells to be active, effector T-cells.

Immunohistochemical staining (IHC) was performed to detect DC-SIGN<sup>+</sup> cells as described previously (Fallert & Reinhart, 2002; Reinhart *et al.*, 2002) using anti-DC-SIGN mAb (clone DCN46; BD Pharmingen). Stained cells were counted at five different sites in the paracortex and the average of the values were taken. Because DC-SIGN is not a completely specific marker for DCs, observing dendritic morphology of most of the stained cells provided confidence that DCs were counted. IHC to detect CD3<sup>+</sup> T-cells was performed similarly and counted in five different microscopic fields and the average of the values were taken.

In all cases, cell counts per volume of tissue were calculated by multiplying the cell count mm<sup>-2</sup> of tissue by the thickness of the tissue section (14 µm) and scaling to appropriate units (ml<sup>-1</sup>).

**In situ hybridization.** *In situ* hybridization was performed as described previously (Fallert & Reinhart, 2002; Reinhart *et al.*, 2002). The numbers of SIV vRNA<sup>+</sup> cells in 10–20 different microscopic fields per region were manually counted and the average of the values were taken.

**Mathematical model.** Our mathematical model describes cell–virus interactions within the paracortical region of a human LN by using a system of nine non-linear ordinary differential equations. These equations describe the rates of flow as cells arrive, interact, change phenotype and exit. Fig. 1 outlines the key features. Each of the biological interactions described below is captured by a mathematical term in our model. A more detailed description and biological justification of the model is given in Supplementary Material (available in JGV Online).

**CD4<sup>+</sup> T-cell dynamics.** We considered three phenotypic classes of CD4<sup>+</sup> T-cells: resting, activated effector and infected. Resting CD4<sup>+</sup> T-cells arrive by infection-independent and -dependent mechanisms. Resting cells can become productively infected, or become abortively infected and undergo apoptosis (Jekle *et al.*, 2003). CD4<sup>+</sup> T-cells are primed by DCs to become effector T-helper cells. A fraction are infected during priming (Lekkerkerker *et al.*, 2006). Activated T-helper cells undergo clonal expansion. T-helper cells can become infected by virus or virus-loaded DCs. Infection is inhibited by CTLs (Geiben-Lynn, 2002). Infected CD4<sup>+</sup> T-cells can be killed by CTLs. All CD4<sup>+</sup> classes can exit via efferent lymphatics.

**HIV-1 dynamics.** Virus is produced by infected CD4<sup>+</sup> T-cells. Production is inhibited by CTL-produced factors (Geiben-Lynn, 2002; Kedzierska & Crowe, 2001; Levy, 2003). The vast majority of virus particles are associated with follicular DCs (Haase, 1999), which extend their half-life (Cavert *et al.*, 1997). Follicular DCs are not explicitly considered here, though we account for their effect on virus half-life.

**CD8<sup>+</sup> T-cell dynamics.** We considered two classes of CD8<sup>+</sup> T-cells: resting and activated effector. Resting CD8<sup>+</sup> T-cells arrive due to infection-independent and -dependent mechanisms. Because CD8<sup>+</sup> T-cells require more (or different) co-stimulatory signals to become fully activated CTLs (Whitmire & Ahmed, 2000), these are primed only by licensed DCs. Primed CTLs undergo clonal expansion. All CD8<sup>+</sup> classes can exit via efferent lymphatics.

**DC dynamics.** Immature DCs arrive independently of infection and mature DCs arrive during infection. Within the LN, immature DCs can encounter antigen and undergo maturation. Mature DCs become licensed through interactions with activated T-helper cells (Ridge *et al.*, 1998). Mature and licensed DCs are susceptible to being killed by CTLs (Ronchese & Hermans, 2001; Yang *et al.*, 2006). Any of these DC classes can die, though mature and licensed DCs are short-lived compared with immature DCs (Ruedl *et al.*, 2000).

**Parameter estimation.** Parameters are estimated from a variety of published sources. For details of parameter estimation, see Supplementary Material. We handled uncertainties in parameter estimation systematically by uncertainty and sensitivity analysis (see below).

**Initialization of the simulation.** Prior to infection, the LN is assumed to contain only resting/immature cells. We determined the initial numbers from immunohistochemistry measures of uninfected NHPs herein, and from published CD4:CD8 ratios (Biancotto *et al.*, 2007). HIV-1 infection dynamics begin with the arrival of a single mature DC at day 0 presenting both viral antigen and infectious virus.

**Solving the model system.** The system of differential equations is solved using the ode15s algorithm in MATLAB (Shampine & Reichelt, 1997). The solution of the system at any given time point yields the average number of each type of cell/virion within the LN. We solved our system over a time course representing years.

**Model validation.** To validate the behaviour of our model, we compared data from our model simulations to NHP SIV-infection data. Our model simulates paracortical LN tissue over a longitudinal time course. However, the invasiveness of LN biopsy makes a longitudinal NHP study difficult. Thus, our experimental data are cross-sectional and categorical. Due to variability between outbred animals, categorization by time post-infection is not completely reliable. Instead, we categorized infection state not only by time post-infection but also by plasma viral load, blood CD4<sup>+</sup> T-cell counts and clinical symptoms. We mapped our experimental animal study categories to ranges of time in our model simulation, for the purpose of comparison.

We additionally validated our model by comparison to published human HIV-1 infection data. We scaled human total-body cell count estimates by 1/700 to represent 1 ml of lymphoid tissue. This conversion assumes typical human body weight is 70 kg, 1% by weight is lymphoid tissue (Haase, 1999) and tissue density is 1 g ml<sup>-1</sup>.

**Uncertainty and sensitivity analysis.** Parameters that govern the rates of interaction in our model are estimated from a variety of published biological data. Because of variability between experimental systems, all estimates have an associated degree of uncertainty. We addressed this uncertainty in a systematic manner by uncertainty and sensitivity analysis. This analysis also determines which parameters are most important in governing the state of the system. Analysis was performed using Latin Hypercube Sampling and Partial Rank Correlation (LHS/PRC) (Blower & Dowlatabadi, 1994; Marino *et al.*, 2008), and the extended Fourier Amplitude Sensitivity Test (eFAST) (Marino *et al.*, 2008; Saltelli *et al.*, 1999). LHS/PRC was performed using 1000 model simulations, and eFAST was performed using 697 simulations per parameter and 6 × parameter resampling for a total of 175 644 model simulations. Briefly, both algorithms sample input parameters independently over a range (see Supplementary Table S1 available in JGV Online). We sampled using a uniform probability distribution function, and sampled on a log scale if the sampling range was two orders of magnitude or greater. The algorithms then performed model simulations with each parameter combination, and measured the sensitivity of the system to changes in each parameter. Like ANOVA, the eFAST method decomposes variance in model output to determine the fraction of variance in model output explained by each input parameter. The eFAST total-order sensitivity index, which we report here, takes into account higher-order interactions between multiple parameters. We determined the limit of detection by allowing the eFAST algorithm to partition variance to a dummy parameter that does not affect model output. To determine statistical significance we perform two-sample Student's *t*-test on eFAST values from parameter resampling. LHS/PRC reports sensitivity as a coefficient of correlation between input parameter and model output. Statistical significance of these correlations was determined by Student's *t*-test with Bonferroni correction (Curran-Everett, 2000). Statistical comparison between these correlation coefficients was performed using Fisher's *z* transformation (Meng *et al.*, 1992). For a complete discussion of uncertainty and sensitivity analysis, see Marino *et al.* (2008).

**In silico interventions.** To explore the role of particular interactions or mechanisms, we performed *in silico* interventions by changing parameter values during the course of a simulation. *In silico* intervention is analogous to altering particular interactions *in vivo* using pharmacological treatments. The flexibility of our *in silico*

system allows us to perform an intervention even if there is no analogous experimental treatment.

In addition, we used *in silico* intervention to induce depletion of CD8<sup>+</sup> T-cells: we blocked recruitment and proliferation, so that no new cells entered the population. Maturation and exit are left in place so that CD8<sup>+</sup> T-cells are gradually depleted. This *in silico* depletion is analogous to experiments where antibodies are used to deplete CD8<sup>+</sup> T-cells from SIV-infected *Rhesus macaques*. A number of groups have demonstrated that this treatment causes a dramatic rise in viral load 1–3 orders of magnitude, depletion of CD4<sup>+</sup> T-cells and disease progression (Jin *et al.*, 1999; Matano *et al.*, 1998; Schmitz *et al.*, 1999). As a positive control, we depleted CD8<sup>+</sup> T-cells *in silico*. For the purpose of our model analysis, we defined an 'AIDS-like state' based on this immunity-impaired positive control.

## RESULTS

To explore the role of DCs during HIV-1 infection, we first captured the homeostatic mechanisms of a healthy LN in the absence of virus. Next, we introduced virus to simulate an acute phase and chronic state of infection, and validated our model by comparing our simulations to SIV-infected NHP data and published human clinical data. Finally, we analysed our model using uncertainty and sensitivity analysis techniques to identify mechanisms involved in HIV-1 infection and pathogenesis.

### Simulation of a healthy LN

As a negative control, we simulated a healthy LN in the absence of virus. By construction, all cell types remained constant in number, reflecting an assumption of homeostasis in the absence of antigen (Doherty & Christensen, 2000). These levels observed in our simulation agreed with NHP infection data derived herein and also with published human clinical data (Haase, 1999) (Table 1).

### Simulation of acute phase and chronic steady-state match human and NHP infection data

Solving the model simulates the populations of each cell type and virus over time (Fig. 2). From our model, we

**Table 1.** Model simulation values compared with NHP experimental data and published human clinical data in LN

Infection state/model time point	Count	Model simulation	NHP	Human clinical data (Haase, 1999)
No infection/day 0	Total CD4 <sup>+</sup> T-cell	3.5 × 10 <sup>8</sup>	3.7 × 10 <sup>8*</sup>	2.9 × 10 <sup>8</sup>
Chronic/day 300	Total CD4 <sup>+</sup> T-cell	8.6 × 10 <sup>7</sup>	10.7 × 10 <sup>7*</sup>	6.7 × 10 <sup>7</sup>
Acute/day 6	Infected cell	2.5 × 10 <sup>6</sup>	1.7 × 10 <sup>6</sup>	7.1 × 10 <sup>5</sup>
Chronic/day 300	Infected cell	8.2 × 10 <sup>5</sup>	6.4 × 10 <sup>5</sup>	5.7 × 10 <sup>4</sup>
Acute/day 6	Virus	2.0 × 10 <sup>9</sup>		>10 <sup>8</sup>
Chronic/day 300	Virus	8.3 × 10 <sup>8</sup>		

\*This value was calculated from total T-cell count and the CD4:CD8 ratio from (Biancotto *et al.*, 2007).

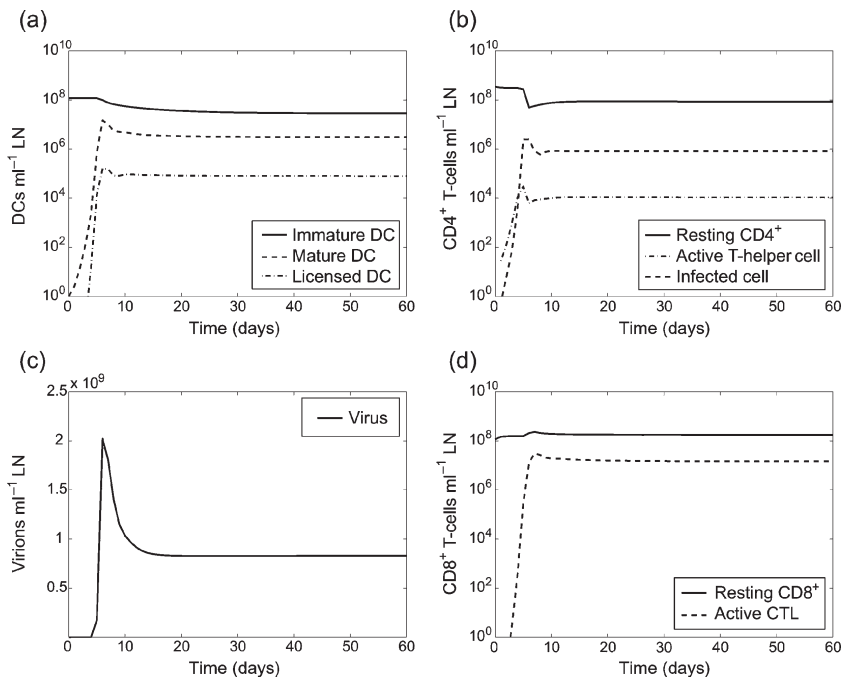


**Fig. 2.** Model simulation shows acute infection settling into chronic infection by day 20. Shown are time courses for all cell types and virus as follows: (a) DCs, (b)  $CD4^+$  T-cells, (c) viral load and (d)  $CD8^+$  T-cells.

calculated experimentally relevant variables for comparison to our NHP experimental data (Fig. 3a–d). We found that our model quantitatively recapitulates the depletion of DCs and T-cells (Fig. 3a and b), and the increase in infected and activated T-cell populations (Fig. 3c and d) in the paracortical regions of an LN during uninfected, acute and chronic infection.

Other studies have shown that DCs are depleted during simian AIDS (Brown *et al.*, 2007). Similarly, we found that total DCs became depleted during SIV infection, both in our experimental animal studies and our model simulations (Fig. 3a). The model simulation predicted that DC depletion occurred gradually after infection peaks (Fig. 3, compare a and c).

Because our model distinguished  $CD4^+$  from  $CD8^+$  T-cells, but our experimental data only measured total T-cells, we additionally validated the model simulation  $CD4:CD8$  ratio by comparison to published HIV-1-infected human LN data (Biancotto *et al.*, 2007). Typically in the blood, the  $CD4:CD8$  ratio inverts from 2:1 to 1:2 over the course of infection (Margolick *et al.*, 2006). However, our model recapitulates the 4:1 to 1:2 inversion of the  $CD4:CD8$  ratio that occurs in human lymphoid tissue during chronic HIV-1 infection (Fig. 3e).

To ensure relevance to human disease, we additionally validated our model simulation by comparison to published human HIV-1 infection data (Table 1). Our model agreed with estimated cell counts of human lymphoid tissue.

### Determination of parameters that drive viral load

Sensitivity and uncertainty analysis revealed how variation in model parameters affected infection dynamics. First, we

analysed parameters directly related to  $CD4^+$  T-cells,  $CD8^+$  T-cells and virus (see Supplementary Material). Next, we found that many of the significant parameters identified by this analysis were DC related (Table 2). These DC-related mechanisms are either positively or negatively correlated with viral load by LHS/PRC, indicating the dual role of DCs in promoting both infection and immunity. We found that the parameter governing the immigration of mature DCs, which have encountered antigen in the periphery ( $\phi_{DM}$ ) has a negative correlation with viral load. Although additional mature DCs promote infection, the net effect is to promote immunity, reducing steady-state viral load. The parameters that control licensing of DCs by T-helper cells ( $\lambda$ ) and priming of CTLs by licensed DCs ( $r_{8L}$ ) are both strongly negatively correlated with viral load as these mechanisms promote immunity. In contrast, parameters that control priming and subsequent infection of T-helper cells by DC-associated virus ( $r_{DM}$  and  $k_{DM}$  respectively) are correlated with increased viral load.

### Importance of DC-facilitated infection varies during the course of HIV-1 infection

Our model captures four mechanisms leading to productive infection of  $CD4^+$  T-cells (Fig. 4a). Resting  $CD4^+$  T-cells become infected cells by all four routes. In the first case, virus infects resting T-cells directly without a need for priming. Of these cells, a small fraction are stimulated to become productively infected and the rest remain abortively infected and undergo apoptosis. This is the only route of infection described that is completely independent of DCs. In the second case,  $CD4^+$  T-cells are concurrently primed and infected by DCs. Cases 3 and 4 depend on

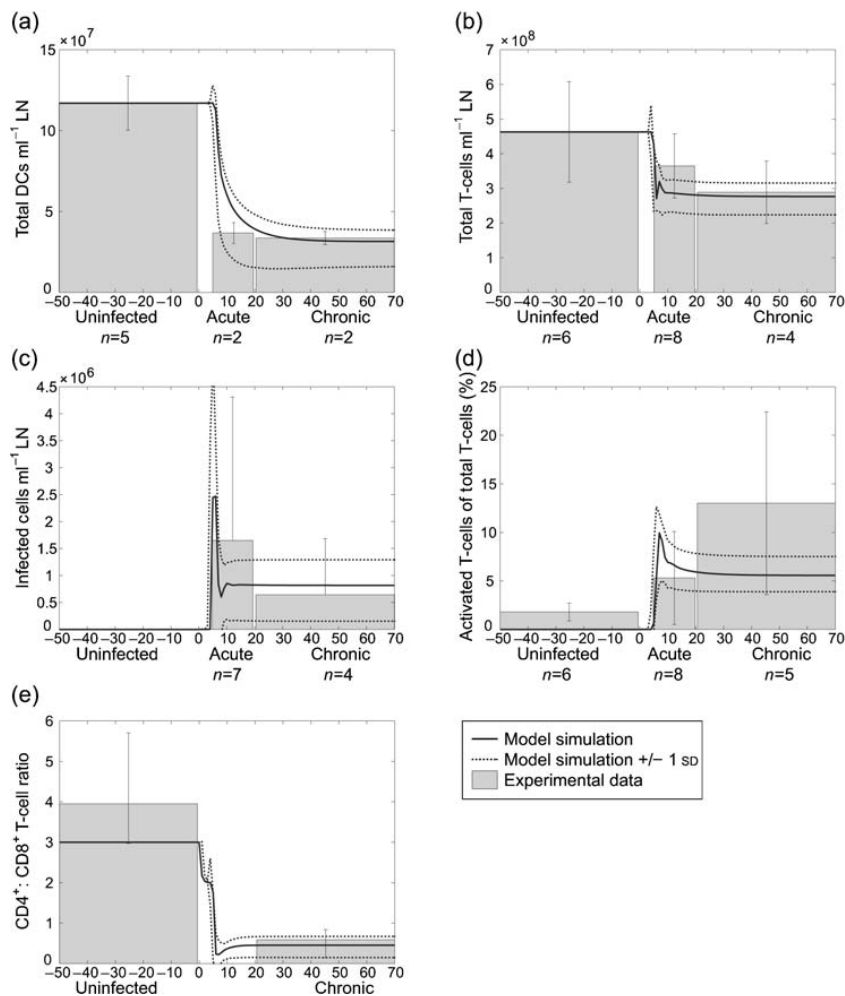


**Fig. 3.** Comparison of model simulation to experimental NHP LN paracortical cell counts, and published human LN data (Biancotto *et al.*, 2007). Model simulation values are derived from Fig. 2. Dotted lines indicate  $\pm 1$  sd of the median of uncertainty analysis simulations. Error bars on experimental data represent 1 sd of the mean. (a) DCs, (b) total T-cells, (c) infected cells, (d) per cent activated T-cell counts and (e) simulation CD4:CD8 T-cell ratio compared with human clinical data from Biancotto *et al.* (2007).

mature or licensed DCs to first prime CD4<sup>+</sup> T-cells. In the third case, virus infects activated T-helper cells independently of DCs. In the fourth case, DC-associated virus infects primed T-helper cells. To gauge the relative importance of each of these infection mechanisms, we performed a focused sensitivity analysis on these nine parameters during establishment of infection/early acute phase and chronic state of infection. During the acute phase of infection, four parameters were significantly correlated with viral load (see asterisks, Fig. 4b): abortive infection of T-cells ( $k_{ab}$ ), which are then stimulated to become productively infected ( $\alpha$ ), priming of T-helper cells ( $r_{DM}$ ), and concurrent priming and infection by mature DCs ( $b_M$ ) were significantly correlated with viral load. During the earliest establishment of infection, there has not been sufficient time to prime many T-helper cells. Thus, mechanisms that require a pool of activated T-helper host cells (such as  $k_V$ ,  $k_{DM}$  and  $k_{DL}$ ) cannot contribute significantly to infection levels. Comparing the relative strength of each of these four infection mechanisms during infection establishment, we found that priming of T-helper cells, and concurrent priming and infection by mature DCs have a significantly greater correlation with viral load than

the other infection mechanisms (see daggers, Fig. 4b). Our model predicted that the ability of DCs to concurrently prime and infect resting CD4<sup>+</sup> T-cells is crucial to the establishment of infection.

During the chronic state of infection (Fig. 4c), abortive infection of resting T-cells becomes negatively correlated, and concurrent priming and infection of T-cells by DCs become insignificant. Instead, infection mechanisms 3 and 4, priming followed by infection (controlled by parameters  $k_V$ ,  $k_{DM}$  and  $k_{DL}$ ), were significantly correlated with chronic state viral loads (see asterisks, Fig. 4c). Comparing the relative significance of each of these mechanisms, we found that infection of activated T-helper cells by DC-associated virus has a significantly greater correlation, revealing the importance of DCs enhancing infection during maintenance of infection (see dagger, Fig. 4c).

### Many mechanisms can cause progression to an AIDS-like state

As a positive control, we depleted CTLs *in silico* (Fig. 5). In the absence of immune effector functions, the system

**Table 2.** Sensitivity and uncertainty analysis identifies parameters that drive viral load

max, Maximum; mat, matured; lic, licensed.

Parameter definition	Symbol	Correlation with viral load†	Sensitivity†
<b>Sensitivity of DC parameters during chronic state</b>			
Recruitment			
Max. immigration rate of mat. DC due to antigen	$\phi_{DM}$	↓	
Licensing			
Licensing rate of mat. DCs by T-helper	$\lambda$	↓	
Priming			
Priming rate of naïve CD4 <sup>+</sup> by mat. DC	$r_{DM}$	↑	
Priming rate of naïve CD8 <sup>+</sup> by lic. DC	$r_{8L}$	↓	
Enhancement of CD4 <sup>+</sup> T-cell infection			
Infection rate of T-helper by mat. DC-associated virus	$k_{DM}$	↑	
<b>Global sensitivity analysis identifies mechanisms that can cause progression to an AIDS-like state</b>			
Source and recruitment			
Max. recruitment rate of naïve CD4 <sup>+</sup> by DC	$\phi_4$		**
Max. recruitment rate of naïve CD8 <sup>+</sup> by DC	$\phi_8$		↓ ↓ **
Max. immigration rate of mat. DC due antigen	$\phi_{DM}$		**
Death/exit to efferent lymph			
Death/exit rate of infected cells	$\mu_I$		↑ ↑
Destruction rate of virus particles	$\mu_V$		↓ ↓ **
Death/exit rate of naïve CD8 <sup>+</sup>	$\mu_8$		↑ ↑
Death/exit rate of CTL	$\mu_C$		↑ ↑
Proliferation/clonal expansion			
Proliferation rate of CTL	$p_C$		↓ ↓
Priming			
Priming rate of naïve CD4 <sup>+</sup> by mat. DC	$r_{DM}$		↑ ↑ **
Priming rate of naïve CD8 <sup>+</sup> by lic. DC	$r_{8L}$		↓ ↓ **
Infection			
Abortive infection and bystander effects of naïve CD4 <sup>+</sup>	$k_{ab}$		↓ ↓ **
Infection rate of T-helper by virus	$k_V$		↑ ↑
Infection rate of T-helper by mat. DC-associated virus	$k_{DM}$		↑ ↑
Virus properties			
Average number of virus produced by an infected cell	$n$		↑ ↑ **
CTL effector functions			
Inhibition of mat. DC-associated virus infection by CTL	$c_2$		↑ ↑
Inhibition of infected cell virus production by CTL	$c_4$		↑ ↑
Killing rate of infected cells by CTL	$\kappa_I$		↓ ↓ **
Killing rate of lic. DC by CTL	$\kappa_L$		↑ ↑
DC maturation and licensing			
Licensing rate of mat. DCs by T-helper	$\lambda$		↓ ↓ **

↑ Statistically significant positive correlation ( $P < 5.9 \times 10^{-4}$ ).

↓ Statistically significant negative correlation ( $P < 5.9 \times 10^{-4}$ ).

† Numerical correlations are given in Supplementary Material (available in JGV Online).

↑↑ Significant positive correlation by LHS/PRC ( $P < 2.4 \times 10^{-4}$ ).

↓↓ Significant negative correlation by LHS/PRC ( $P < 2.4 \times 10^{-4}$ ).

\*\* Significant total-order sensitivity index by eFAST ( $P < 0.01$ ).

†† Numerical sensitivity indices are given in Supplementary Material (available in JGV Online).

established a new steady-state characterized by a high viral load set-point (Fig. 5a and b, bold solid line) and reduction in CD4<sup>+</sup> T-cell counts (not shown). In subsequent model analysis, we compared the effects of other *in silico* interventions to this positive control ‘AIDS-like state’.

The parameters we found to be significant in our sensitivity analysis (Table 2) are important in determining viral load. Thus, mechanisms controlled by these parameters are likely involved, singly or in combination, in the transition to AIDS. Specific parameters identified by both LHS/PRC and

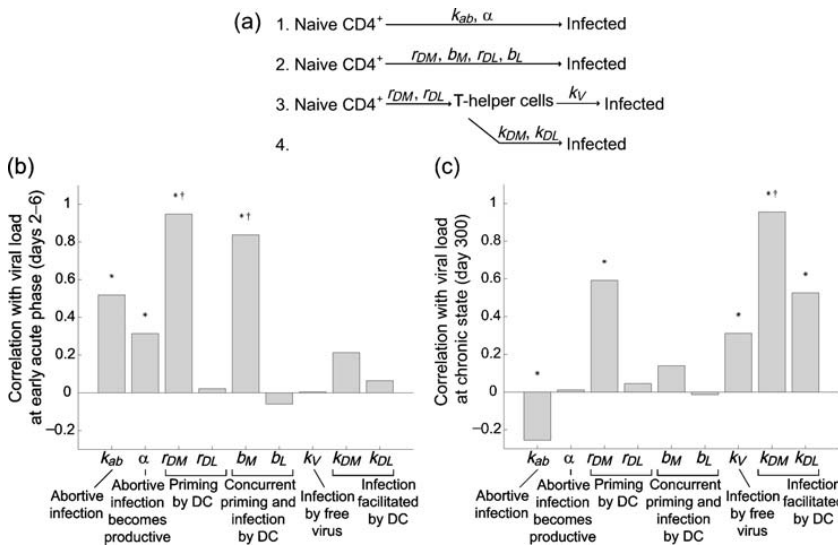


**Fig. 4.** Sensitivity analysis on different routes of infection. (a) Four mechanisms of infection were captured by the model. (b) Correlation between parameter value and early acute phase viral load (days 2–6). (c) Correlation between parameter value and chronic-state viral load (day 300). (\*= $P < 0.0011$ ) (†=significantly different from all other parameters  $P < 0.0003$ ).

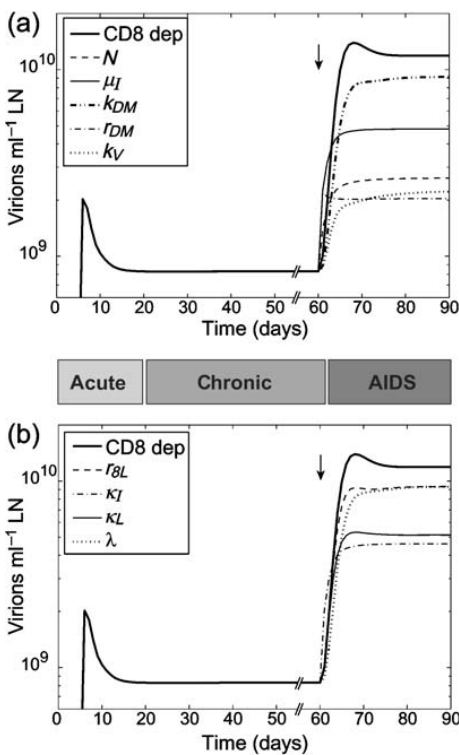


**Fig. 5.** Parameters that induce an AIDS-like state. Parameters are increased or reduced to the extremes of their range of variation (see Supplementary Table S1) at day 60 (see arrow) to determine whether they are capable of inducing an AIDS-like state. In both panels, an AIDS-like state is induced by CD8<sup>+</sup> T-cell depletion at day 60 (see arrow), as a positive control. All other parameters are held to their default values (see Supplementary Table S1). (a) Parameters related to infection and viral production. (b) Parameters related to immune effector functions. Table 2 accompanies this figure and presents all the parameters and their definitions.

eFAST methods have a very significant effect on viral load. However, the relative strengths and weaknesses of these algorithms cause them to identify different subsets of marginally sensitive parameters. These statistically significant but weak mechanisms might work in combination with each other, or the more significant mechanisms, causing a multi-factorial progression to AIDS. To test which mechanisms could be involved in progression to an AIDS-like state, we performed *in silico* intervention by varying the mechanisms that were identified in the sensitivity analysis (Fig. 5). We found that parameters that were able to cause an AIDS-like state fell into three functional categories: first, mechanisms related to infection and viral replication (Fig. 5a); second, mechanisms related to maintenance or effector functions of immune response (Fig. 5b); and third, mechanisms related to death or exit of CD8<sup>+</sup> T-cells or virus (Supplementary Fig. S2). As expected, based on DCs dual roles, DC functions are represented in the infection (Fig. 5a) and immune response (Fig. 5b) categories.

The first functional group of parameters identified ( $N, \mu_I, k_{DM}, r_{DM}$  and  $k_V$ ) was related to mechanisms of infection and viral replication. Changing these parameters from their baseline values to the extremes of their range of variation (see Supplementary Table S1) can induce a transition to an AIDS-like state. This supports the hypothesis that a progressive adaptation of virus could result in progression to AIDS. Adaptation of virus has been suggested by others: mechanisms include changes in co-receptor usage or affinity (Gorry *et al.*, 2004; Xiao *et al.*, 1998), or increases in replication number (Stilianakis *et al.*, 1997). In addition, it has been shown that the HIV-1 protein Nef causes upregulation of DC-SIGN in infected DCs, possibly increasing DC-enhanced infection (Sol-Foulon *et al.*, 2002).

The second functional group of parameters ( $r_{\beta L}, \kappa_I, \kappa_L$  and  $\lambda$ ) controls maintenance or effector functions of immune

response. Three of these mechanisms form a causal pathway: first, DCs become licensed by T-helper cells ( $\lambda$ ); next, licensed DCs prime CTLs ( $r_{8L}$ ); and finally: CTLs kill infected T-cells ( $\kappa_I$ ). We found that reducing any of these mechanisms to the minimum of their range of variation (see Supplementary Table S1) results in a failure of the immune response to control infection, leading to an AIDS-like state. This finding lends support to the hypothesis that an impairment of immune response results in an inability to control viral load. Immunologically, reduction in CTL priming or CTL killing of infected cells could result from the acquisition of CTL epitope mutations (Wodarz & Nowak, 2002). Alternatively, as DCs are central to the generation of CTL response, alterations in licensed DC function could impair immunity.

The third functional group identified, parameters related to death or exit of  $CD8^+$  T-cells or virus, represents mechanisms related to lymphoid tissue architecture and regulated traffic of cells through LNs. This finding is not surprising given that alterations in T-cell migration and LN architecture are hallmarks of HIV-1 infection, other chronic infections and immunodeficiency in general (von Andrian & Mempel, 2003). See Supplementary Material for details on these results.

Finally, we found that statistically significant but weakly correlated parameters ( $\phi_4, \phi_8, \phi_{DM}, p_C, c_2$  and  $c_4$ ) were unable to independently induce an AIDS-like viral load. Because components of the immune system are highly interactive, progressive HIV-1 infection to AIDS is likely a multi-factorial and multi-step process. Indeed, we find that these parameters in combination can lead to an increase in viral load approximately equal to acute phase viraemia (Supplementary Fig. S2 available in JGV Online).

### DC dysfunction in progression to AIDS

Two main hypotheses exist for the role of DC dysfunction in progression to AIDS (Fig. 6a). The first suggests that, as T-helper cells become depleted by HIV-1 infection, they are present in insufficient numbers to license DCs, which in turn reduces the ability of DCs to prime  $CD8^+$  T-cells. The second hypothesis suggests that DC dysfunction is the result of a direct viral effect on DC intracellular processes (Chougnnet & Gessani, 2006; Cohen *et al.*, 1999). Likely, both mechanisms are at play during infection; however, our model analysis tests if one hypothesis is more significant in the progression to AIDS. To this end, we varied parameters controlling DC licensing by T-helper cells ( $\lambda$ ) and licensed DC priming of CTLs ( $r_{8L}$ ). When all other confounding factors are held constant at their default parameter values (Supplementary Table S1) we found that decreasing either or both of these mechanisms can cause an AIDS-like viral load. To examine further, we used global sensitivity analysis using the eFAST method to perform thousands of *in silico* experiments varying all model parameters simultaneously. This analysis identifies overall sensitivities that were apparent despite uncertainty or

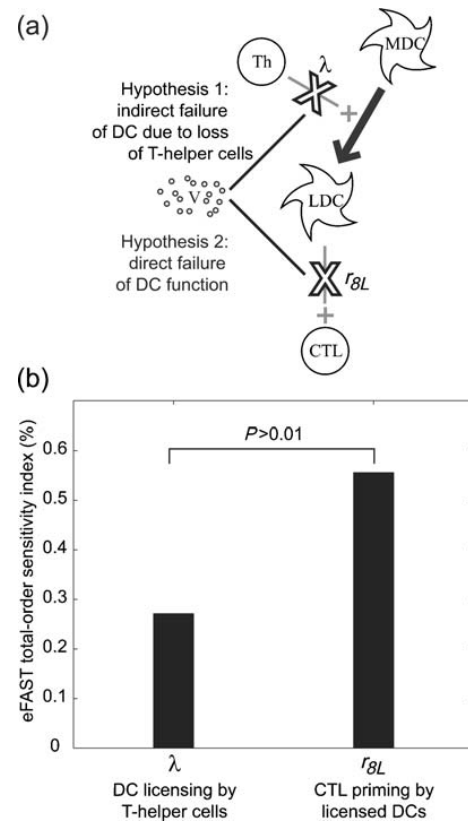


**Fig. 6.** Direct failure of licensed DCs is more likely to contribute to HIV-1 immunopathogenesis than an indirect failure of  $CD4^+$  T-helper cells. (a) Two hypotheses of DC dysfunction: loss of  $CD4^+$  T-helper cells could indirectly cause DC failure to prime CTLs (hypothesis 1). This is represented in the model by a decrease in parameter  $\lambda$ . Alternatively, the virus could directly impair DC function (hypothesis 2). This is represented in the model by a decrease in parameter  $r_{8L}$ . (b) Global sensitivity analysis using the eFAST method shows that CTL priming by licensed DCs ( $r_{8L}$ ) is a significantly more sensitive control point of the system, favouring hypothesis 2.

variability in other mechanisms. We found that licensed DC priming of CTLs ( $r_{8L}$ ) was a significantly more sensitive ( $P < 0.01$ ) control point than DC licensing by T-helper cells ( $\lambda$ ). This result indicates that, given biological variability in many other mechanisms affecting both DCs and CTLs, a direct failure of licensed DCs is more likely to contribute to HIV-1 immunopathogenesis than an indirect failure of  $CD4^+$  T-helper cells to license DCs. This finding suggests that therapies targeting DC function will be more successful than therapies targeting a failure of  $CD4^+$  T-helper cells, as this is a stronger control point of the system.

### DISCUSSION

The immune response to infectious disease is complex: the individual cells of the immune system are highly interact-

ive, and the overall function of the system is a product of this multitude of interactions. The interplay between HIV-1 and the immune system is particularly complicated, as HIV-1 directly interacts with many immune cells, altering their functions, ultimately subverting the system at its core. Because of this complexity, the immune response and its interaction with HIV-1 are naturally suited to a mathematical modelling approach. Building on previous work (Bajaria & Kirschner, 2005; Bajaria *et al.*, 2002), we present, to our knowledge, the first mechanistic model of the specific roles of DCs during HIV-1 infection. Here, we focus on the dynamics within an LN and the role of different classes of DCs in HIV-1 dynamics. We moved beyond the 'Langerhan's cell paradigm' of DC function by including LN-resident immature DCs and multiple maturation/activation states. We focused on LN, as it is the nexus of viral replication and antiviral immune response, and is historically under studied due to difficulties in observing human lymphoid tissue. Further, the LN has been consistently under appreciated in mathematical models studying HIV-1 infection and immune system dynamics.

Sensitivity and uncertainty analysis reveals which parameters and, by extension, which interactions are most important in determining the function of the virus–host system. Our analysis shows that many of the most important parameters that determine viral load levels relate to DCs. This finding illustrates the role of DCs as a central hub of interaction and information exchange during HIV-1 infection.

Others have suggested that the immune system has evolutionarily optimized 'bow-tie' or 'hour-glass' structural motifs, in which diverse and redundant input signals converge on a single control point. The signals are integrated and produce diverse and redundant output signals to the rest of the system. They suggest that CD4<sup>+</sup> T-cells serve as one control point, and propose that the severity of AIDS results from HIV-1 compromising this vulnerable control point (Kitano & Oda, 2006). Similarly, our results show that DCs serve as a control point: DCs integrate signals from the pathogen and other components of the immune system, then signal other immune system cells by way of MHC molecules, co-stimulation and cytokines.

Given the central position of DCs in immune system interactions, it is not surprising that HIV-1 has adapted to exploit them to enhance infection. We showed that this enhancement is important in maintaining chronic infection viral load levels, and that increasing this effect can induce progression to an AIDS-like state. Others have suggested that the ability of HIV to infect resting CD4<sup>+</sup> T-cells is critical for the earliest stage of infection, as resting T-cells predominate in the peripheral tissue where HIV is first encountered (Zhang *et al.*, 2004). Importantly, we found a similar phenomenon when HIV arrives in an LN: in the early stages, when activated T-helper cells are

limited, concurrent priming and infection by DCs is crucial in driving acute viraemia.

We also explored the opposing antiviral immunogenic role of DCs. We showed that T-helper cells for DC licensing, priming of CTLs by licensed DCs and CTL killing of infected cells are all critical steps in controlling chronic infection. Impairing any of these steps can cause an AIDS-like state. In particular, our model analysis suggests that the system as a whole is more sensitive to the direct failure of DCs to prime CTLs, rather than by the indirect route of failure of T-helper cells to DCs. This finding has implications for the design of therapeutic vaccines and adjuvants: modulation of DC numbers and function could improve the outcome of infection, even if other immunological defects cannot be treated.

One limitation of this kind of model is that differential equations consider average rates of interaction between populations. The model cannot capture stochastic effects or spatial heterogeneity. Ongoing work includes agent-based models of immune response in an LN that addresses these issues (Riggs *et al.*, 2008).

Clearly experimental science has made vast advances in the study of the immune response and, in particular, HIV-1 infection dynamics. The systems biology approach presented here lends an additional tool to guide our understanding of the complexities of this biological system. An integrative approach can be most useful for identifying factors that are crucial to infection outcomes, and here we have presented multiple predictions that can now be further explored in an experimental setting.

## ACKNOWLEDGEMENTS

We thank Jenna Vanliere for early efforts on this work, and members of the Kirschner Lab for helpful discussions. Dawn McClemens-McBride, Anita Trichel, Julia Nyaundi and Michael Murphey-Corb assisted with animal studies. S. Watkins, J. Devlin and S. Albert assisted with the confocal microscopy and analysis.

## REFERENCES

- Arrighi, J. F., Pion, M., Garcia, E., Escola, J. M., van Kooyk, Y., Geijtenbeek, T. B. & Piguet, V. (2004). DC-SIGN-mediated infectious synapse formation enhances X4 HIV-1 transmission from dendritic cells to T cells. *J Exp Med* **200**, 1279–1288.
- Bajaria, S. H. & Kirschner, D. (2005). CTL action during HIV-1 is determined via interactions with multiple cell types. In *Deterministic and Stochastic Models for AIDS Epidemics and HIV Infection with Interventions*, pp. 219–254. Edited by W. Y. Tan & H. Wu. River Edge, NJ: World Scientific.
- Bajaria, S. H., Webb, G., Cloyd, M. & Kirschner, D. (2002). Dynamics of naive and memory CD4<sup>+</sup> T lymphocytes in HIV-1 disease progression. *J Acquir Immune Defic Syndr* **30**, 41–58.
- Biancotto, A., Grivel, J. C., Iglehart, S. J., Vanpouille, C., Lisco, A., Sieg, S. F., Debernardo, R., Garate, K., Rodriguez, B. & other authors (2007). *Abnormal Activation and Cytokine Spectra in Lymph Nodes of Persons Chronically Infected with HIV-1. Blood*.

- Blauvelt, A., Asada, H., Saville, M. W., Klaus-Kovtun, V., Altman, D. J., Yarchoan, R. & Katz, S. I. (1997).** Productive infection of dendritic cells by HIV-1 and their ability to capture virus are mediated through separate pathways. *J Clin Invest* **100**, 2043–2053.
- Blower, S. M. & Dowlatabadi, H. (1994).** Sensitivity and uncertainty analysis of complex models of disease transmission: an HIV model, as an example. *Int Stat Rev* **62**, 229–243.
- Brown, K. N., Trichel, A. & Barratt-Boyes, S. M. (2007).** Parallel loss of myeloid and plasmacytoid dendritic cells from blood and lymphoid tissue in simian AIDS. *J Immunol* **178**, 6958–6967.
- Bukczynski, J., Wen, T., Wang, C., Christie, N., Routy, J. P., Boulassel, M. R., Kovacs, C. M., Macdonald, K. S., Ostrowski, M. & other authors (2005).** Enhancement of HIV-specific CD8 T cell responses by dual costimulation with CD80 and CD137L. *J Immunol* **175**, 6378–6389.
- Cavert, W., Notermans, D. W., Staskus, K., Wietgreffe, S. W., Zupancic, M., Gebhard, K., Henry, K., Zhang, Z. Q., Mills, R. & other authors (1997).** Kinetics of response in lymphoid tissues to antiretroviral therapy of HIV-1 infection. *Science* **276**, 960–964.
- Choungnet, C. & Gessani, S. (2006).** Role of gp120 in dendritic cell dysfunction in HIV infection. *J Leukoc Biol* **80**, 994–1000.
- Cohen, S. S., Li, C., Ding, L., Cao, Y., Pardee, A. B., Shevach, E. M. & Cohen, D. I. (1999).** Pronounced acute immunosuppression *in vivo* mediated by HIV Tat challenge. *Proc Natl Acad Sci U S A* **96**, 10842–10847.
- Cohen Stuart, J. W., Hazebergh, M. D., Hamann, D., Otto, S. A., Borleffs, J. C., Miedema, F., Boucher, C. A. & de Boer, R. J. (2000).** The dominant source of CD4+ and CD8+ T-cell activation in HIV infection is antigenic stimulation. *J Acquir Immune Defic Syndr* **25**, 203–211.
- Curran-Everett, D. (2000).** Multiple comparisons: philosophies and illustrations. *Am J Physiol Regul Integr Comp Physiol* **279**, R1–R8.
- Dioszeghy, V., Benlhassan-Chahour, K., Delache, B., Dereuddre-Bosquet, N., Aubenque, C., Gras, G., Le Grand, R. & Vaslin, B. (2006).** Changes in soluble factor-mediated CD8+ cell-derived antiviral activity in cynomolgus macaques infected with simian immunodeficiency virus SIVmac251: relationship to biological markers of progression. *J Virol* **80**, 236–245.
- Doherty, P. C. & Christensen, J. P. (2000).** Accessing complexity: the dynamics of virus-specific T cell responses. *Annu Rev Immunol* **18**, 561–592.
- Fallert, B. A. & Reinhart, T. A. (2002).** Improved detection of simian immunodeficiency virus RNA by *in situ* hybridization in fixed tissue sections: combined effects of temperatures for tissue fixation and probe hybridization. *J Virol Methods* **99**, 23–32.
- Geiben-Lynn, R. (2002).** Anti-human immunodeficiency virus noncytolytic CD8+ T-cell response: a review. *AIDS Patient Care STDS* **16**, 471–477.
- Gorry, P. R., Sterjovski, J., Churchill, M., Witlox, K., Gray, L., Cunningham, A. & Wesselingh, S. (2004).** The role of viral coreceptors and enhanced macrophage tropism in human immunodeficiency virus type 1 disease progression. *Sex Health* **1**, 23–34.
- Granelli-Piperno, A., Golebiowska, A., Trumppheller, C., Siegal, F. P. & Steinman, R. M. (2004).** HIV-1-infected monocyte-derived dendritic cells do not undergo maturation but can elicit IL-10 production and T cell regulation. *Proc Natl Acad Sci U S A* **101**, 7669–7674.
- Haase, A. T. (1999).** Population biology of HIV-1 infection: viral and CD4+ T cell demographics and dynamics in lymphatic tissues. *Annu Rev Immunol* **17**, 625–656.
- Hazenbergh, M. D., Stuart, J. W., Otto, S. A., Borleffs, J. C., Boucher, C. A., de Boer, R. J., Miedema, F. & Hamann, D. (2000).** T-cell division in human immunodeficiency virus (HIV)-1 infection is mainly due to immune activation: a longitudinal analysis in patients before and during highly active antiretroviral therapy (HAART). *Blood* **95**, 249–255.
- Ho, D. D. (1996).** Viral counts count in HIV infection. *Science* **272**, 1124–1125.
- Janeway, C. (2005).** *Immunobiology: The Immune System in Health and Disease*, 6th edn. New York: Garland Science.
- Janssen, E. M., Lemmens, E. E., Wolfe, T., Christen, U., von Herrath, M. G. & Schoenberger, S. P. (2003).** CD4+ T cells are required for secondary expansion and memory in CD8+ T lymphocytes. *Nature* **421**, 852–856.
- Jekle, A., Keppler, O. T., De Clercq, E., Schols, D., Weinstein, M. & Goldsmith, M. A. (2003).** *In vivo* evolution of human immunodeficiency virus type 1 toward increased pathogenicity through CXCR4-mediated killing of uninfected CD4 T cells. *J Virol* **77**, 5846–5854.
- Jin, X., Bauer, D. E., Tuttleton, S. E., Lewin, S., Gettie, A., Blanchard, J., Irwin, C. E., Safrit, J. T., Mittler, J. & other authors (1999).** Dramatic rise in plasma viremia after CD8+ T cell depletion in simian immunodeficiency virus-infected macaques. *J Exp Med* **189**, 991–998.
- Kedzierska, K. & Crowe, S. M. (2001).** Cytokines and HIV-1: interactions and clinical implications. *Antivir Chem Chemother* **12**, 133–150.
- Kitano, H. & Oda, K. (2006).** Robustness trade-offs and host-microbial symbiosis in the immune system. *Mol Syst Biol* **2**, 0022.
- Krathwohl, M. D., Schacker, T. W. & Anderson, J. L. (2006).** Abnormal presence of semimature dendritic cells that induce regulatory T cells in HIV-infected subjects. *J Infect Dis* **193**, 494–504.
- Kwon, D. S., Gregorio, G., Bitton, N., Hendrickson, W. A. & Littman, D. R. (2002).** DC-SIGN-mediated internalization of HIV is required for trans-enhancement of T cell infection. *Immunity* **16**, 135–144.
- Lekkerkerker, A. N., van Kooyk, Y. & Geijtenbeek, T. B. (2006).** Viral piracy: HIV-1 targets dendritic cells for transmission. *Curr HIV Res* **4**, 169–176.
- Levy, J. A. (2003).** The search for the CD8+ cell anti-HIV factor (CAF). *Trends Immunol* **24**, 628–632.
- Margolick, J. B., Gange, S. J., Detels, R., O’Gorman, M. R., Rinaldo, C. R., Jr & Lai, S. (2006).** Impact of inversion of the CD4/CD8 ratio on the natural history of HIV-1 infection. *J Acquir Immune Defic Syndr* **42**, 620–626.
- Marino, S., Hogue, I. B., Ray, C. J. & Kirschner, D. E. (2008).** A methodology for performing global uncertainty and sensitivity analysis in systems biology. *J Theor Biol* (in press)..
- Matano, T., Shibata, R., Siemon, C., Connors, M., Lane, H. C. & Martin, M. A. (1998).** Administration of an anti-CD8 monoclonal antibody interferes with the clearance of chimeric simian/human immunodeficiency virus during primary infections of rhesus macaques. *J Virol* **72**, 164–169.
- McDonald, D., Wu, L., Bohks, S. M., KewalRamani, V. N., Unutmaz, D. & Hope, T. J. (2003).** Recruitment of HIV and its receptors to dendritic cell-T cell junctions. *Science* **300**, 1295–1297.
- Mellman, I. & Steinman, R. M. (2001).** Dendritic cells: specialized and regulated antigen processing machines. *Cell* **106**, 255–258.
- Meng, X., Rosenthal, R. & Rubin, D. B. (1992).** Comparing correlated correlation coefficients. *Psychol Bull* **111**, 172–175.
- Murphey-Corb, M., Martin, L. N., Rangan, S. R., Baskin, G. B., Gormus, B. J., Wolf, R. H., Andes, W. A., West, M. & Montelaro, R. C. (1986).** Isolation of an HTLV-III-related retrovirus from macaques with simian AIDS and its possible origin in asymptomatic mangabeys. *Nature* **321**, 435–437.

- Pitcher, C. J., Hagen, S. I., Walker, J. M., Lum, R., Mitchell, B. L., Maino, V. C., Axthelm, M. K. & Picker, L. J. (2002). Development and homeostasis of T cell memory in rhesus macaque. *J Immunol* **168**, 29–43.
- Poli, G., Pantaleo, G. & Fauci, A. S. (1993). Immunopathogenesis of human immunodeficiency virus infection. *Clin Infect Dis* **17** (Suppl. 1), S224–S229.
- Reimann, K. A., Parker, R. A., Seaman, M. S., Beaudry, K., Beddall, M., Peterson, L., Williams, K. C., Veazey, R. S., Montefiori, D. C. & other authors (2005). Pathogenicity of simian-human immunodeficiency virus SHIV-89.6P and SIVmac is attenuated in cynomolgus macaques and associated with early T-lymphocyte responses. *J Virol* **79**, 8878–8885.
- Reinhart, T. A., Fallert, B. A., Pfeifer, M. E., Sanghavi, S., Capuano, S., III, Rajakumar, P., Murphey-Corb, M., Day, R., Fuller, C. L. & Schaefer, T. M. (2002). Increased expression of the inflammatory chemokine CXC chemokine ligand 9/monokine induced by interferon-gamma in lymphoid tissues of rhesus macaques during simian immunodeficiency virus infection and acquired immunodeficiency syndrome. *Blood* **99**, 3119–3128.
- Ridge, J. P., Di Rosa, F. & Matzinger, P. (1998). A conditioned dendritic cell can be a temporal bridge between a CD4<sup>+</sup> T-helper and a T-killer cell. *Nature* **393**, 474–478.
- Riggs, T., Walts, A., Perry, N., Bickle, L., Lynch, J. N., Myers, A., Flynn, J., Linderman, J. J., Miller, M. J. & Kirschner, D. E. (2008). A comparison of random vs. chemotaxis-driven contacts of T cells with dendritic cells during repertoire scanning. *J Theor Biol* **250**, 732–751.
- Ronchese, F. & Hermans, I. F. (2001). Killing of dendritic cells: a life cut short or a purposeful death? *J Exp Med* **194**, F23–F26.
- Ruedl, C., Koebel, P., Bachmann, M., Hess, M. & Karjalainen, K. (2000). Anatomical origin of dendritic cells determines their life span in peripheral lymph nodes. *J Immunol* **165**, 4910–4916.
- Saltelli, A., Tarantola, S. & Chan, K. P.-S. (1999). A quantitative model-independent method for global sensitivity analysis of model output. *Technometrics* **41**, 39–56.
- Schmitz, J. E., Kuroda, M. J., Santra, S., Sasseville, V. G., Simon, M. A., Lifton, M. A., Racz, P., Tenner-Racz, K., Dalesandro, M. & other authors (1999). Control of viremia in simian immunodeficiency virus infection by CD8<sup>+</sup> lymphocytes. *Science* **283**, 857–860.
- Schoenberger, S. P., Toes, R. E., van der Voort, E. I., Offringa, R. & Melief, C. J. (1998). T-cell help for cytotoxic T lymphocytes is mediated by CD40–CD40L interactions. *Nature* **393**, 480–483.
- Serre, K., Giraud, L., Siret, C., Leserman, L. & Machy, P. (2006). CD4 T cell help is required for primary CD8 T cell responses to vesicular antigen delivered to dendritic cells in vivo. *Eur J Immunol* **36**, 1386–1397.
- Shampine, L. F. & Reichelt, M. W. (1997). The MATLAB ODE Suite. *SIAM J Sci Comput* **18**, 1–22.
- Shedlock, D. J. & Shen, H. (2003). Requirement for CD4 T cell help in generating functional CD8 T cell memory. *Science* **300**, 337–339.
- Smith, C. M., Wilson, N. S., Waithman, J., Villadangos, J. A., Carbone, F. R., Heath, W. R. & Belz, G. T. (2004). Cognate CD4<sup>+</sup> T cell licensing of dendritic cells in CD8<sup>+</sup> T cell immunity. *Nat Immunol* **5**, 1143–1148.
- Sol-Foulon, N., Moris, A., Nobile, C., Boccaccio, C., Engering, A., Abastado, J. P., Heard, J. M., van Kooyk, Y. & Schwartz, O. (2002). HIV-1 Nef-induced upregulation of DC-SIGN in dendritic cells promotes lymphocyte clustering and viral spread. *Immunity* **16**, 145–155.
- Steinman, R. M. (1991). The dendritic cell system and its role in immunogenicity. *Annu Rev Immunol* **9**, 271–296.
- Stilianakis, N. I., Dietz, K. & Schenzle, D. (1997). Analysis of a model for the pathogenesis of AIDS. *Math Biosci* **145**, 27–46.
- Trepel, F. (1974). Number and distribution of lymphocytes in man. A critical analysis. *Klin Wochenschr* **52**, 511–515.
- Turville, S. G., Cameron, P. U., Handley, A., Lin, G., Pohlmann, S., Doms, R. W. & Cunningham, A. L. (2002). Diversity of receptors binding HIV on dendritic cell subsets. *Nat Immunol* **3**, 975–983.
- von Andrian, U. H. & Mempel, T. R. (2003). Homing and cellular traffic in lymph nodes. *Nat Rev Immunol* **3**, 867–878.
- Wang, J. C. & Livingstone, A. M. (2003). Cutting edge: CD4<sup>+</sup> T cell help can be essential for primary CD8<sup>+</sup> T cell responses *in vivo*. *J Immunol* **171**, 6339–6343.
- Whitmire, J. K. & Ahmed, R. (2000). Costimulation in antiviral immunity: differential requirements for CD4<sup>+</sup> and CD8<sup>+</sup> T cell responses. *Curr Opin Immunol* **12**, 448–455.
- Wilson, N. S. & Villadangos, J. A. (2004). Lymphoid organ dendritic cells: beyond the Langerhans cells paradigm. *Immunol Cell Biol* **82**, 91–98.
- Wodarz, D. & Nowak, M. A. (2002). Mathematical models of HIV pathogenesis and treatment. *Bioessays* **24**, 1178–1187.
- Xiao, L., Rudolph, D. L., Owen, S. M., Spira, T. J. & Lal, R. B. (1998). Adaptation to promiscuous usage of CC and CXC-chemokine coreceptors in vivo correlates with HIV-1 disease progression. *AIDS* **12**, F137–F143.
- Yang, J., Huck, S. P., McHugh, R. S., Hermans, I. F. & Ronchese, F. (2006). Perforin-dependent elimination of dendritic cells regulates the expansion of antigen-specific CD8<sup>+</sup> T cells *in vivo*. *Proc Natl Acad Sci U S A* **103**, 147–152.
- Zhang, Z. Q., Wietgreffe, S. W., Li, Q., Shore, M. D., Duan, L., Reilly, C., Lifson, J. D. & Haase, A. T. (2004). Roles of substrate availability and infection of resting and activated CD4<sup>+</sup> T cells in transmission and acute simian immunodeficiency virus infection. *Proc Natl Acad Sci U S A* **101**, 5640–5645.

PAPER vir83600

Please quote this number in any correspondence

Authors I. B. Hogue and others

Date \_\_\_\_\_

I would like 25 free offprints, plus  additional offprints, giving a total of  offprints

Dispatch address for offprints (BLOCK CAPITALS please)

---



---



---

Please complete this form **even if you do not want extra offprints**. Do not delay returning your proofs by waiting for a purchase order for your offprints: the offprint order form can be sent separately.

Please pay by credit card or cheque with your order if possible. Alternatively, we can invoice you. All remittances should be made payable to 'Society for General Microbiology' and crossed 'A/C Payee only'.

Tick one

- Charge my credit card account (give card details below)
- I enclose a cheque/draft payable to Society for General Microbiology
- Purchase order enclosed

Return this form to: JGV Editorial Office, Marlborough House, Basingstoke Road, Spencers Wood, Reading RG7 1AG, UK.

#### CHARGES FOR ADDITIONAL OFFPRINTS

Copies	25	50	75	100	125	150	175	200	Per 25 extra
No. of pages									
1-2	£23	£40	£58	£76	£92	£110	£128	£145	£23
3-4	£35	£58	£81	£104	£128	£150	£173	£191	£29
5-8	£46	£76	£104	£133	£162	£191	£219	£249	£35
9-16	£58	£92	£128	£162	£196	£231	£267	£301	£40
17-24	£70	£110	£151	£191	£231	£272	£312	£353	£46
each 8pp extra	£18	£23	£29	£35	£40	£46	£53	£58	

#### OFFICE USE ONLY

Issue:
Vol/part:
Page nos:
Extent:
Price:
Invoice: IR/

#### PAYMENT BY CREDIT CARD (Note: we cannot accept American Express)

Please charge the sum of £\_\_\_\_\_ to my credit card account.

My Mastercard/Visa number is (circle appropriate card; no others acceptable):

<input type="text"/>	<input type="text"/>	<input type="text"/>	<input type="text"/>
----------------------	----------------------	----------------------	----------------------

Expiry  
date

<input type="text"/>	<input type="text"/>
----------------------	----------------------

Security  
Number

<input type="text"/>	<input type="text"/>
----------------------	----------------------

Signature: \_\_\_\_\_ Date: \_\_\_\_\_

Cardholder's name and address\*: \_\_\_\_\_

\*Address to which your credit card statement is sent. Your offprints will be sent to the address shown at the top of the form.